(IJCSNT) International Journal of Communication Systems and Network Technologies
ISSN Number: 2053-6283
Volume 13, Issue No. 3, 159–171
©The Author(s) 2024
https://journals.mirlabs.in/index.php/ijcsnt
DOI-10.18486/ijcsnt/13.3.185
IJCSNT

Compact UWB Textile Antenna with Multi-Phase Evolution from Single to Dual Designs

D Ramesh Varma[1], K Padma Vasavi[2], M Padmini Chowdary[3], M Venkata Subbarao[4], G Challa Ram[5], D Girish Kumar[6]

Abstract
In this paper, the design and performance analysis of ultra-wideband (UWB) antennas employing flexible textile substrates are presented for wearable wireless communication systems. A three-phase design strategy is adopted, beginning with a single antenna element, followed by a dual-element configuration, and finally a stub-coupled dual arrangement to mitigate mutual coupling and improve impedance bandwidth. Textile materials including nylon, leather, cotton, and silk are utilized as dielectric substrates, and their impact on impedance characteristics, resonance behavior, and bandwidth is systematically investigated. The reflection coefficient S11 results demonstrate that substrate permittivity and dielectric losses play a crucial role in shaping antenna performance. Silk and nylon substrates exhibit deeper resonances with good impedance matching, while leather provides broader operating bandwidth. Cotton, due to its higher dielectric loss, yields comparatively shallow resonances and reduced efficiency. For dual-element designs, mutual coupling effects are evident, but the incorporation of a central stub significantly enhances port isolation, maintaining S11< -10dB across the 3.1–10.6 GHz UWB band. The antennas also maintain stable radiation patterns, acceptable gain, and conformal robustness under bending conditions. The proposed textile-based UWB antenna designs confirm the feasibility of low-cost, flexible, and reliable solutions for wearable and body-centric communication applications, with the stub-coupled configuration demonstrating superior performance among the investigated cases.

Keywords
Ultra-wideband Antenna, Textile Antenna, Wearable Communication, Stub-coupled Configuration

Received: 17 August 2024; **Revised:** 30 November 2024; **Accepted:** 14 December 2024; **Published:** 31 December 2024;

[1, 2, 3, 4, 5, 6]Department of ECE, Shri Vishnu Engineering College for Women (A), Bhimavaram, Andhra Pradesh, India.

Corresponding author:
Email: varmaramesh422@svecw.edu.in

Introduction

This In modern wireless communication, multiple-input multiple-output (MIMO) systems have gained significant attention due to their ability to enhance channel capacity and mitigate performance degradation caused by multipath fading. Ultra-wideband (UWB) technology, on the other hand, has emerged as a promising candidate for high-speed, low-power data transmission over a broad frequency spectrum. However, UWB systems are inherently affected by multipath fading resulting from diffraction and reflection between closely placed antennas, which can be effectively addressed through the incorporation of MIMO techniques[1,2]. Compact and high-performance wearable antennas are increasingly demanded in various domains, including disaster management, health monitoring, medical diagnostics, telemedicine, fitness tracking, and satellite communication systems[3,4]. With its advantages of low cost, high data rate, and short-range capability, UWB is considered an attractive solution for on-body wireless networks, where propagation challenges in body-centric communication remain an active research area[5]. To meet the requirements of such applications, antennas must be miniaturized, multiband, and capable of reliable performance in compact devices[6].

MIMO architectures contribute significantly to improving link reliability and reducing interference by exploiting spatial diversity[7,8]. The integration of MIMO with UWB is therefore viewed as a viable strategy to overcome the inherent limitations of standalone UWB communication[9–11]. Moreover, MIMO systems can achieve higher channel capacity without requiring additional spectrum or increased transmit power[12]. Textile antennas provide a practical platform for wearable applications due to their flexibility, conformability, and ease of integration into clothing[13]. Nevertheless, designing antennas on the human body poses challenges, as the lossy and high-permittivity nature of body tissues tends to degrade radiation efficiency[14]. This necessitates careful consideration of antenna placement, material choice, and integration strategies to achieve optimal performance[4,15–17]. Notably, textile materials usually exhibit low dielectric constants, which help reduce surface wave losses while simultaneously improving impedance bandwidth, making them suitable candidates for wearable UWB antenna designs. Wearable antennas fabricated on textile substrates are generally larger in size compared to those implemented on high-permittivity materials. Their design must also account for practical challenges such as twisting, folding, bending, and exposure to washing cycles[18,19]. In MIMO systems, the use of multiple antennas significantly enhances spectral efficiency at both the transmitter and receiver; however, this advantage is maximized only when the spatial correlation among signals from different antenna elements remains low[20]. Increasing the number of antenna elements improves spatial multiplexing capability, but the proximity of closely spaced elements introduces strong mutual coupling, which in turn degrades MIMO performance due to higher channel correlation. One straightforward way to mitigate this coupling is to increase the inter-element spacing, but this compromises the compactness of the design. Therefore, dedicated decoupling and isolation techniques are preferred, as they enable higher isolation without increasing the overall antenna footprint[21]. Several methods have been proposed to enhance the performance of MIMO antennas including defected ground structures (DGS), split-ring resonators (SRR), stubs, slots, and electromagnetic bandgap (EBG) structures which are effective in improving gain, bandwidth, and port isolation[22,23]. Among these, minimizing mutual coupling remains a critical design requirement, since a low envelope correlation coefficient (ECC) is essential to achieving high diversity gain (DG).

The development of wearable MIMO antennas is especially valuable for practical environments where reliability, robustness, and wideband performance are required. Although various wearable MIMO antennas with reduced coupling have been reported, none have been specifically optimized for UWB operation. Consequently, the design of UWB MIMO antennas that provide broad impedance bandwidth, high gain, low ECC, and stable radiation characteristics is of considerable research and application interest.

In this study, an UWB antenna is proposed in three distinct configurations. The design begins with a single-element antenna, is extended to a dual-element structure, and finally evolves into a stub-coupled dual configuration to improve isolation and reduce mutual coupling. Textile substrates including nylon, cotton, silk, and leather are employed to investigate their effect on antenna performance in terms of return loss, impedance bandwidth, radiation efficiency, and conformal robustness. The reflection characteristics S11 demonstrate that substrate permittivity and dielectric loss significantly influence antenna behavior: silk and nylon yield deep resonances, leather supports broader coverage, while cotton shows limited bandwidth due to higher dielectric loss. Furthermore, the introduction of a stub between the dual antennas enhances port isolation, achieving S11< -10 dB across the 3.1–10.6 GHz band, with stable radiation patterns.

The novelty of this work lies in the systematic three-phase design evolution on textile substrates, coupled with isolation improvement using a stub element, tailored for body-centric communication. The proposed approach demonstrates the feasibility of compact, low-cost, and flexible UWB antennas for next-generation wearable systems, offering reliable performance under real-world conditions.

The paper is structured in a following manner. Section I is about Introduction of ultra-wide band antennas, section II discusses about methodology of the antenna design and presents the dimensions of the proposed antenna, section III deals with result of the simulated antenna and the effects of the parameters on the antenna. section IV gives the conclusion of the work.

Antenna Design Methodology

The design and analysis of the proposed compact UWB microstrip patch antenna were carried out using a structured approach that included substrate selection, radiator design, electromagnetic simulation, and performance validation. A leather-based textile substrate with dimensions of 55 mm $\times$ 35 mm and a thickness of 1.6 mm was employed. The dimensions of the proposed antenna is tabulated in Table I. Leather was selected due to its relatively low dielectric constant and small loss tangent, properties that support improved radiation efficiency while minimizing signal attenuation. Also, analysis is made using different textile substrates like silk, nylon and cotton for understanding of the behaviour of the antenna for different substrates with dielectric constant, loss tangent and different heights. The antenna evolution is performed from single antenna to dual antenna and two antennae with stub between them.

Each configuration was carefully moduled and simulated using full-wave electromagnetic simulation software to evaluate critical performance parameters, including return loss (S11), voltage standing wave ratio, gain, radiation pattern, and surface current distribution across a frequency range of 3 GHz to 10 GHz.

The effective dielectric constant is given as

$$\varepsilon_{eff} = \frac{\varepsilon_r + 1}{2} + \frac{\varepsilon_r - 1}{2}\left(1 + 12\frac{h}{D}\right)^{-1/2} \tag{1}$$

Table 1. TABLE I Dimensions of Proposed Antenna

Parameter	Value(mm)
Length of the Ground	10.5
Width of the Ground	55
Height of the Ground	0.035
Length of the Feed	9.6
Length of the Substrate (Ls)	35
Width of the Substrate (Ws)	55
Height of the Substrate	1.6
Outer Radius of the Patch (R2)	9
Inner Radius of the Patch (R1)	5

Where h is the thickness of the substrate, D is the diameter of the patch and ε_r is the relative permittivity of the substrate.

Corrected effective radius due to fringing fields is given as

$$R_{eff} = R\sqrt{1 + \frac{2h}{\pi\varepsilon_r R}\left(\ln\left(\frac{\pi R}{2h}\right) + 1.7726\right)} \quad (2)$$

In the first design phase, a single octagonal ring-shaped patch antenna is developed on a textile substrate of overall size Ls $\times$ Ws as shown in Fig.1. The radiating element consists of an inner radius (R1) and an outer radius (R2), forming a ring structure that supports multiple resonant modes for ultra-wideband operation. The antenna is excited through a microstrip feed line of length (Lf) and width (Wf), optimized to achieve wide impedance bandwidth and stable matching.

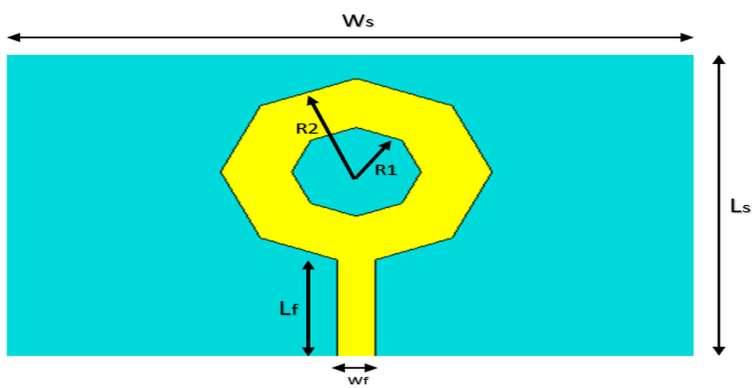

Figure 1. Geometry of the proposed Phase-I single UWB antenna

In the second design phase, a dual-element octagonal ring antenna configuration is developed to explore diversity performance. The two identical radiating patches are placed symmetrically with a center-to-center spacing of 28 mm, resulting in a 10 mm edge-to-edge separation between the elements as shown in Fig.2. Each antenna element maintains the same inner and outer radii as in the Phase-I design,

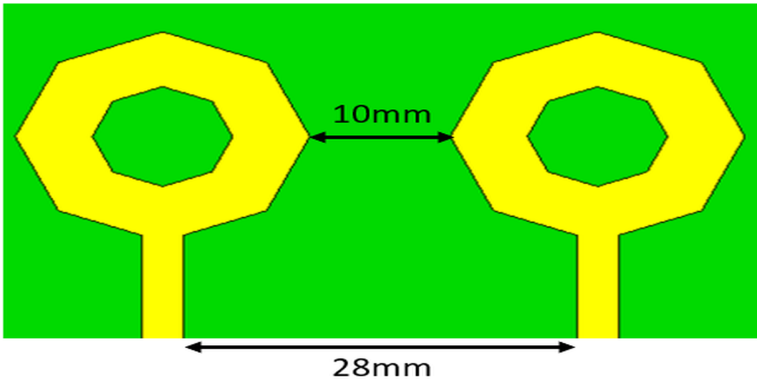

Figure 2. Geometry of the proposed Phase-II dual UWB antenna

while being excited through individual microstrip feed lines. The close proximity of the two elements introduces mutual coupling, which is analysed in terms of return loss and isolation. This configuration serves as the intermediate step toward the stub-coupled design, highlighting the challenges of mutual coupling in compact UWB MIMO antenna systems.

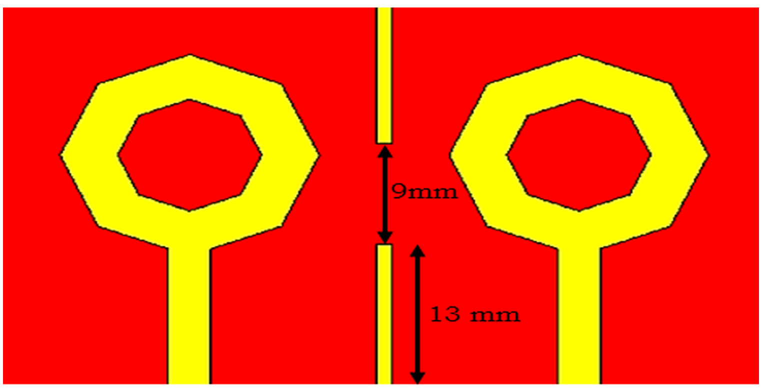

Figure 3. Geometry of the proposed Phase-III dual UWB antenna with isolation stub

In the third design phase, a dual-element circular ring antenna is integrated with a centrally placed vertical stub to mitigate the effects of mutual coupling. The two identical radiating elements are separated by 9 mm, and the stub, with a length of 13 mm, is etched between them on the ground plane as shown in Fig.3. The stub functions as a decoupling structure by suppressing surface currents in the coupling region, thereby enhancing port isolation and reducing channel correlation. This configuration achieves significant improvement in return loss and isolation characteristics compared to the Phase-II design, while maintaining the compactness and wideband operation of the antenna. The stub-coupled structure demonstrates the most effective performance among the three phases, making it a suitable candidate for wearable UWB MIMO systems.

Results and Discussion

Reflection coefficient (S11)

The proposed antenna structures were evaluated in three phases to examine the effect of textile substrates, element configuration, and isolation enhancement on the UWB performance. The results are presented in terms of the reflection coefficient (S11), highlighting the impedance matching behaviour across the 3–12 GHz frequency range.

Figure 4 shows the simulated reflection coefficient of the single-element UWB antenna designed on four different textile substrates: silk, nylon, leather, and cotton. The results indicate that the dielectric properties of the substrates play a crucial role in determining the impedance bandwidth and resonance behavior. Among the substrates considered, silk and nylon demonstrate deeper resonances with S11 values dropping below –30 dB and –25 dB, respectively, around 8 GHz, indicating strong impedance matching. Leather provides a broader bandwidth with resonances extending across the UWB band but at a slightly higher reflection level (around –20 dB). Cotton, owing to its higher dielectric loss, exhibits limited resonance depth and poorer impedance matching, with S11values remaining close to –10 dB across most of the band. These results confirm that leather, nylon, and silk are better substrates for wearable UWB applications, whereas cotton is less effective due to its lossy nature.

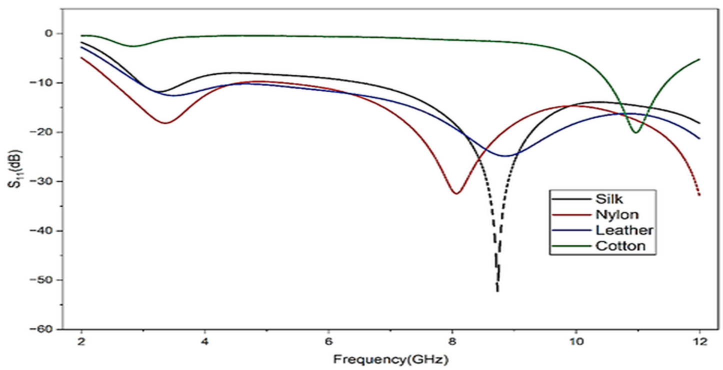

Figure 4. Reflection coefficient of the proposed Phase-I single-element UWB antenna using different textile substrates

In Phase II, the dual-element antenna maintains wideband coverage but suffers from strong mutual coupling, limiting resonance depth and keeping S11 values around –15 dB as shown in Fig.5. This indicates reduced impedance matching and insufficient isolation for MIMO operation.

With the introduction of a central stub in Phase III, the reflection response improves significantly. The stub suppresses surface current interaction, leading to deeper resonances nearly –30 dB for leather and below –20 dB for nylon substrates. This enhancement restores proper impedance matching and improves isolation, making the stub-coupled design far more effective for wearable UWB MIMO applications.

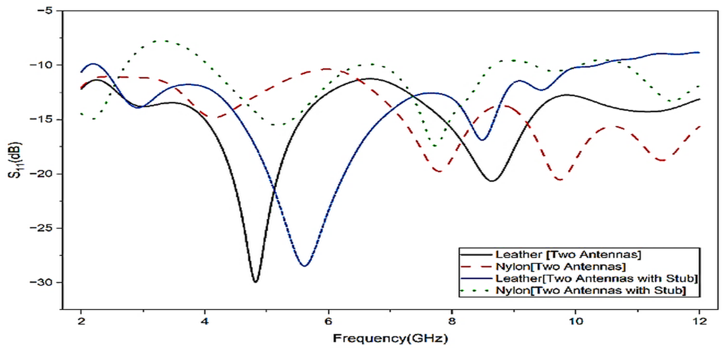

Figure 5. Reflection coefficient comparison of Phase-II dual-element and Phase-III stub-coupled dual-element UWB antenna configurations using leather and nylon substrates.

Voltage Standing Wave Ratio

The Voltage Standing Wave Ratio (VSWR) is an important parameter that reflects how effectively power is delivered from the feed line to the antenna. Lower VSWR values correspond to improved impedance matching and reduced signal reflection. For practical antenna systems, a VSWR below 2 is typically regarded as satisfactory. In UWB antenna design, it is essential to maintain VSWR values under this threshold throughout the operating band to guarantee efficient power transfer, stable radiation, and full utilization of the available bandwidth. Figure 6 illustrates the variation of the VSWR with frequency for the proposed single-element UWB antenna using four textile substrates. A VSWR value below 2 is generally considered acceptable for practical antenna designs, as it corresponds to a return loss better than –10 dB. It is observed that silk, nylon, and leather substrates maintain VSWR values well below 2 across most of the UWB range (3.1–10.6 GHz), confirming good impedance matching and stable wideband performance. In contrast, the cotton substrate exhibits significantly higher VSWR, with values exceeding 10 at several frequencies, indicating poor matching and higher reflection losses. This is attributed to the relatively higher dielectric losses of cotton, which degrade the impedance bandwidth. From figure 6, the results suggest that silk, nylon, and leather are suitable candidates for UWB wearable antennas, while cotton is less suggested due to its poor impedance performance.

Gain of the Antenna

Figure 7 illustrates the gain characteristics of the single-element UWB antenna implemented on different textile substrates. The results indicate that nylon, leather, and silk provide stable gain responses, maintaining values in the range of 3–5 dB across the operating band. In contrast, cotton exhibits lower and less stable gain, with peak values not exceeding 3 dB, which can be attributed to its higher dielectric losses and inferior impedance matching properties.

Figure 8 presents the gain performance for the dual-element (Phase II) and stub-coupled dual-element (Phase III) configurations. The dual-element structure achieves moderate gain levels but shows irregular variations, primarily due to strong mutual coupling between the radiating elements. With the introduction

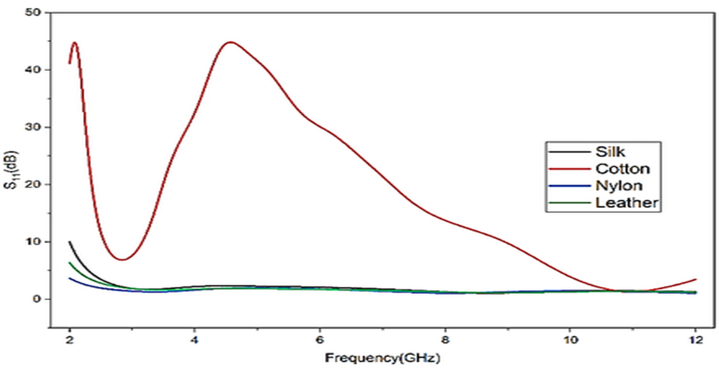

Figure 6. VSWR Analysis for Impedance Matching in UWB Antenna Design

of the isolation stub in Phase III, the antenna demonstrates improved performance, achieving peak gain values exceeding 5 dB and exhibiting a smoother gain response across the UWB spectrum. The enhancement confirms that the stub reduces surface current interaction in the coupling region, thereby improving radiation efficiency without compromising compactness. These results establish that the stub-coupled configuration offers superior gain stability and efficiency compared to the single-element and conventional dual-element designs, validating its suitability for UWB wearable MIMO applications.

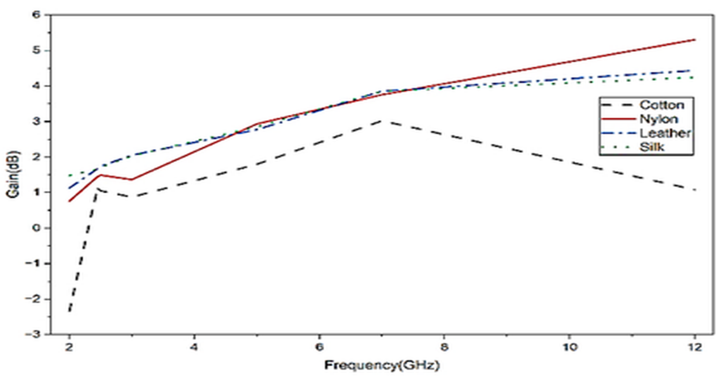

Figure 7. Gain response of the Phase-I single-element UWB antenna with different textile substrates.

Efficiency of the Antenna

Figure 9 presents the total radiation efficiency of the single-element UWB antenna implemented on leather, nylon, and cotton substrates. The results indicate that leather provides the best performance, with efficiency exceeding 80% across the operating band, demonstrating low dielectric loss and stable energy transfer.

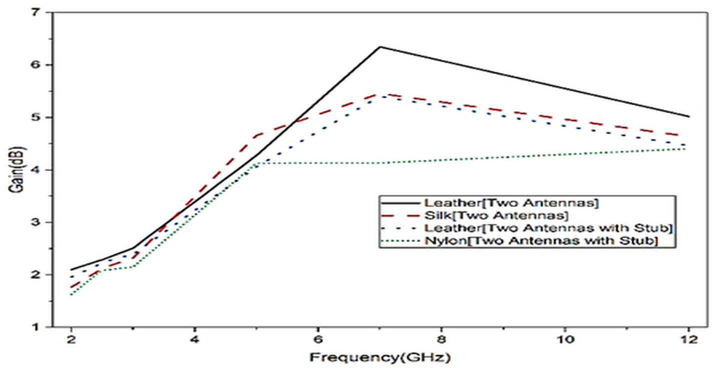

Figure 8. Gain performance of Phase-II dual-element and Phase-III stub-coupled UWB antenna configurations.

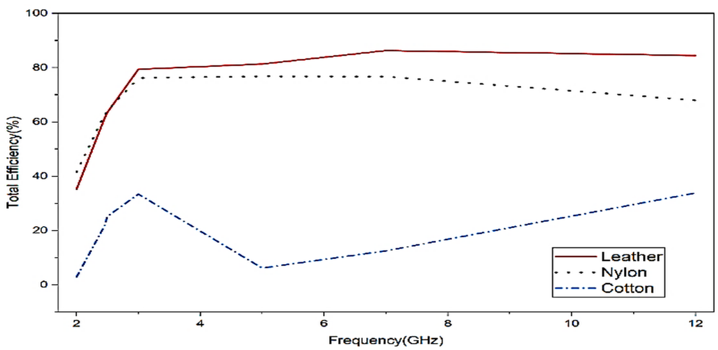

Figure 9. Total radiation efficiency of the Phase-I single-element UWB antenna with textile substrates.

Nylon exhibits slightly lower efficiency, remaining in the range of 70–75%, which is still adequate for UWB wearable communication. In contrast, cotton shows poor performance, with efficiency values dropping below 30% for most of the band and large fluctuations at higher frequencies.

Surface Currents and Field Patterns of the Antenna

Figure 10 illustrates the surface current distribution of the dual-element UWB antenna without and with the isolation stub. In the absence of the stub, strong surface currents are observed along both radiating elements, as well as in the coupling region between them. This confirms the presence of significant mutual coupling, which adversely affects port isolation and impedance matching.

When the stub is introduced between the two elements, the surface current density in the coupling region is significantly reduced. The stub effectively suppresses unwanted current flow between the elements, thereby improving isolation and minimizing correlation between the antenna ports. This redistribution of currents validates the improvement in return loss, gain stability, and overall efficiency observed in the stub-coupled design. Figure 11 shows the field patterns of the proposed antenna for the stub design.

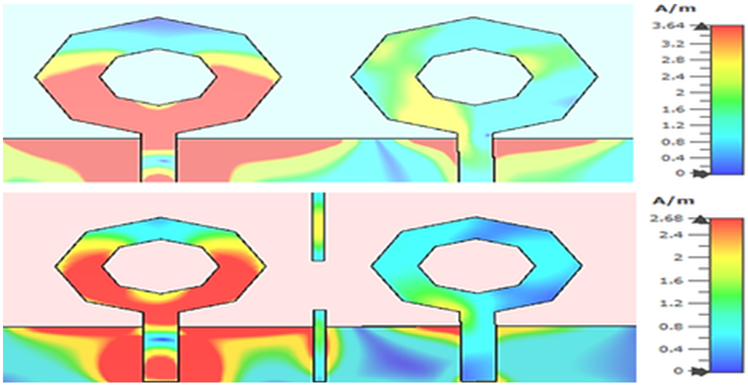

Figure 10. Surface current distribution of the dual-element UWB antenna

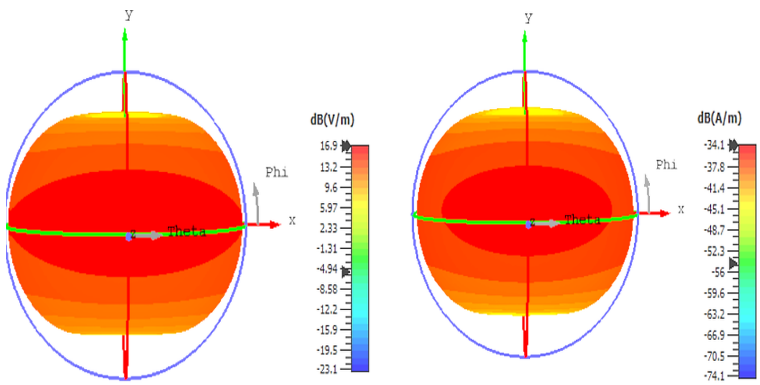

Figure 11. Electric Field and Magnetic Field of proposed antenna

Conclusion

In this work, a compact UWB antenna was designed and analysed through a three-phase development process: a single-element configuration, a dual-element structure, and a stub-coupled dual-element design. The performance of the proposed antenna was evaluated on various textile substrates, including leather, nylon, silk, and cotton, to assess their suitability for wearable communication systems. The results demonstrated that leather and nylon provided stable impedance matching, high efficiency, and consistent gain, whereas cotton exhibited poor performance due to its higher dielectric losses. The dual-element configuration highlighted the limitations of mutual coupling in compact UWB MIMO antennas.

Table 2. Table II Comparison of the Proposed Antenna with Recently Reported UWB MIMO Designs

Design	Board size (mm^2)	No. of elements	Substrate dielectric constant	Max. gain	Gap between elements (mm)	Port isolation (dB)
[1]	45 × 45	4	FR4, 4.4	3 dB	6	>17
[8]	22 × 26	2	FR4, 4.4	3.8 dBi	8	>18
[9]	25 × 30	2	FR4, 4.4	5.2 dBi	16	>20
[25]	35 × 35	4	FR4, 4.4	Not provided	Not provided	>20
[26]	58 × 58	2	Rogers RT/Duroid 6035HTC, 3.6	2.2 dBi	2.83	>14
[27]	50 × 30	2	FR4, 4.4	4.3 dB	Not provided	>20
Proposed	55 × 35	2	Textile (Leather, Nylon, Silk), 1.6, 1.2	6.9 dB	6	>26

To address this, an isolation stub was introduced, which effectively suppressed surface currents in the coupling region. The stub-coupled design achieved improved port isolation (>26 dB), enhanced gain (up to 6.9 dB), and high efficiency (>80%) across the UWB band. These improvements establish the proposed design as a strong candidate for body-centric and wearable UWB communication systems, where compactness, wideband operation, and high reliability are critical. Future work may focus on experimental validation under dynamic bending and wearable scenarios, as well as exploring advanced decoupling techniques and multi-element extensions for next-generation on-body wireless networks.

References

[1] S. Tripathi, A. Mohan, and S. Yadav, "A compact Koch fractal UWB MIMO antenna with WLAN band rejection," IEEE Antennas and Wireless Propagation Letters, vol. 14, pp. 1565–1568, 2015.

[2] T. Bolin, A. Derneryd, G. Kristensson, et al., "Two antenna receive diversity performance in indoor environment," Electronics Letters, vol. 41, pp. 1205–1206, 2005.

[3] R. V. Dandu, V. S. Mandava, C. R. Grandhi, N. Prasanna, S. Tanniru, and S. S. D. Kameswari, "Design of semi-flexible slotted patch antenna for biomedical applications," in Advanced Technologies in Electronics, Communications and Signal Processing. ICATECS 2024, K. K. Koganti, S. R. E., and N. Gupta, Eds. Cham, Switzerland: Springer, 2026, Lecture Notes of the Institute for Computer Sciences, Social Informatics and Telecommunications Engineering, vol. 619. doi: https://doi.org/10.1007/978-3-031-94280-8_10

[4] D. R. Varma, M. Murali, M. V. Krishna and G. S. N. Raju, "Miniaturized Novel Textile Antenna for Biomedical Applications," 2023 2nd International Conference on Paradigm Shifts in Communications Embedded Systems, Machine Learning and Signal Processing (PCEMS), Nagpur, India, 2023, pp. 1-6, doi: 10.1109/PCEMS58491.2023.10136066.

[5] D. R. Varma, M. Murali, and M. V. Krishna, “Compact, robust and low-profile textile antennas for biomedical applications with upgraded bandwidth for integration of easy garment,” Materials Today: Proceedings, vol. 80, no. 2, pp. 1548–1555, 2023, doi: https://doi.org/10.1016/j.matpr.2023.01.388.

[6] K. Panda, S. Sahu, and R. K. Mishra, “A compact dual-band 2 $\times$ 1 metamaterial inspired MIMO antenna system with high port isolation for LTE and WiMAX applications,” International Journal of RF and Microwave Computer-Aided Engineering, vol. 27, no. 8, p. e21122, 2017.

[7] H. Hussain, A. T. Alreshaid, S. K. Podilchak, et al., “Compact 4G MIMO antenna integrated with a 5G array for current and future mobile handsets,” IET Microwaves, Antennas & Propagation, vol. 11, no. 2, pp. 271–279, 2017.

[8] C. M. Luo, J. S. Hong, and L. L. Zhong, “Isolation enhancement of a very compact UWB MIMO slot antenna with two defected ground structure,” IEEE Antennas and Wireless Propagation Letters, vol. 14, pp. 1766–1769, 2015.

[9] T. K. Roshna, U. Deepak, V. R. Sajitha, et al., “A compact UWB MIMO antenna with reflector to enhance isolation,” IEEE Transactions on Antennas and Propagation, vol. 63, no. 4, pp. 1873–1877, 2015.

[10] M. S. Khan, A. D. Capobianco, A. Iftikhar, et al., “Ultra-compact dual-polarised UWB MIMO antenna with meandered feeding lines,” IET Microwaves, Antennas & Propagation, vol. 11, no. 7, pp. 997–1002, 2017.

[11] W. T. Li, Y. Q. Hei, H. Subbaraman, et al., “Novel printed filtenna with dual notches and good out-of-band characteristics for UWB-MIMO applications,” IEEE Microwave and Wireless Components Letters, vol. 26, no. 10, pp. 765–767, 2016.

[12] S. F. Jilani and A. Alomainy, “Millimetre-wave T-shaped MIMO antenna with defected ground structures for 5G cellular networks,” IET Microwaves, Antennas & Propagation, vol. 12, no. 5, pp. 672–677, 2018.

[13] D. R. Varma, B. D. Saranya, G. Pavani, M. V. Subbarao, G. C. Ram, and D. G. Kumar, “Design of fabric antennas for body protective garment applications and analysis on their performance,” Materials Today: Proceedings, vol. 80, no. 2, pp. 1538–1547, 2023, doi: https://doi.org/10.1016/j.matpr.2023.01.384

[14] D. Wen, Y. Hao, M. O. Munoz, et al., “A compact and low-profile MIMO antenna using a miniature circular high-impedance surface for wearable applications,” IEEE Transactions on Antennas and Propagation, vol. 66, no. 1, pp. 96–104, 2018.

[15] W. A. Ali, A. M. Mansour, and D. A. Mohamed, “Compact UWB wearable planar antenna mounted on different phantoms and human body,” Microwave and Optical Technology Letters, vol. 58, no. 10, pp. 2531–2536, 2016.

[16] Salam, A. A. Khan, and M. S. Hussain, “Dual band microstrip antenna for wearable applications,” Microwave and Optical Technology Letters, vol. 56, no. 4, pp. 2531–2536, 2014.

[17] H. Li, S. Sun, B. Wang, et al., "Design of compact single-layer textile MIMO antenna for wearable applications," IEEE Transactions on Antennas and Propagation, vol. 66, no. 6, pp. 3136–3141, 2018.

[18] N. Singh, A. K. Singh, and V. K. Singh, "Design and performance of wearable ultrawide band textile antenna for medical applications," Microwave and Optical Technology Letters, vol. 57, no. 7, pp. 1553–1557, 2015.

[19] X. Hu, S. Yan, and G. A. E. Vandenbosch, "Wearable button antenna for dual-band WLAN applications with combined on and off-body radiation patterns," IEEE Transactions on Antennas and Propagation, vol. 65, no. 3, pp. 1384–1387, 2017.

[20] R. Tian, V. Plicanic, B. K. Lau, et al., "A compact six-port dielectric resonator antenna array: MIMO channel measurements and performance analysis," IEEE Transactions on Antennas and Propagation, vol. 58, no. 4, pp. 1369–1379, 2010.

[21] R. Saleem, M. Bilal, K. B. Bajwa, et al., "Eight-element UWB-MIMO array with three distinct isolation mechanisms," Electronics Letters, vol. 51, no. 4, pp. 311–313, 2015.

[22] C. J. Malathi and D. Thiripurasundari, "Review on isolation techniques in MIMO antenna systems," Indian Journal of Science and Technology, vol. 9, no. 35, pp. 1–10, 2016.

[23] L. Grau, A. Andújar, and J. Anguera, "On the isolation of a MIMO 2×2 antenna system using non-resonant elements: 1.71 GHz–2.69 GHz case study," Microwave and Optical Technology Letters, vol. 59, no. 6, pp. 2348–2353, 2017.